Available online at www.sciencedirect.com
SCIENCE DIRECT
Polymer 47 (2006) 3954–3960
polymer
www.elsevier.com/locate/polymer

The effect of high-pressure carbon dioxide treatment on the crystallization behavior and mechanical properties of poly(L-lactic acid)/ poly(methyl methacrylate) blends

Shin-ichi Hirota, Takatoshi Sato, Yoichi Tominaga, Shigeo Asai, Masao Sumita *

Department of Chemistry and Materials Science, Tokyo Institute of Technology, 2-12-1 Ookayama, Meguro-ku, Tokyo 152-8550, Japan

Received 10 October 2005; received in revised form 20 January 2006; accepted 18 March 2006
Available online 18 April 2006

Abstract

The purpose of this study is to investigate the effect of carbon dioxide (CO_2) on the crystallization behavior and the mechanical properties of PLLA/PMMA blends with various weight fraction of PMMA. PLLA/PMMA blends can be crystallized even at a low temperature of 0 °C under high-pressure CO_2. The films treated with high-pressure CO_2 at 0 °C have about three times larger strain at break than that of the amorphous and cold-crystallized film. The size of spherulites in the CO_2 treated film is considered to be smaller than the wavelength of the visible light because of a good transparency. The improvement of the strain at break is attributed to the reduction of the stress concentration during the deformation.

Keywords: Polymer blend; Carbon dioxide; Crystallization

1. Introduction

Poly(L-lactic acid) (PLLA), which is known as a biodegradable polymer and synthesized from the raw materials derived from renewable resources, is brought to a lot of attention as a substitute for general-purpose resins because the glass transition temperature (T_g) of PLLA is relatively high among biodegradable polymers and PLLA has a transparency in the amorphous state. However, an improvement of a heat resistance is required to use PLLA as a substitute of general-purpose resins. The suppression of molecular mobility by the crystallization or the addition of fillers leads to inhibition of an abrupt decrease in modulus at the T_g. Blending PLLA with a polymer, which has miscibility with PLLA and has the T_g higher than that of PLLA, shifts the softening temperature to higher temperatures. The combined use of the crystallization method and the blending method is expected to improve still further a heat resistance. A PLLA film crystallized by annealing becomes opaque because of the scattering of the visible light by the crystals in the film. Moreover, the formation of the crystal-amorphous heterogeneous structure causes brittleness because of the stress concentration during the deformation. The crystallization of polymers using high-pressure carbon dioxide (CO_2) is effective to eliminate above weak points. The CO_2 absorbed into polymer increases the free volume and decreases the T_g of the polymer because of enhancement of the molecular mobility. Therefore, a semi-crystalline polymer can be crystallized under high-pressure CO_2 at a low temperature at which the crystallization does not occur in air. Asai et al. studied on the crystallization behavior of poly(ethylene naphthalate) (PEN) under supercritical CO_2 ($scCO_2$) [1]. They reported that the size of the lamellae structure becomes smaller with decreasing the temperature of $scCO_2$ treatment. In general, the nucleation becomes more dominant with decreasing annealing temperature. If the size of spherulites is smaller than the wavelength of visible light, a semi-crystalline polymer can be crystallized without losing a transparency. In addition, the miniaturization of the heterogeneous structure leads to avoid the stress concentration during the deformation. Poly(methyl methacrylate) (PMMA) is an amorphous polymer with a good transparency and has the T_g higher than that of PLLA. Zhang et al. reported that PMMA has miscibility with PLLA in molten state and the two polymers were miscible even after quenching from the melt [2]. Therefore, blending PLLA and PMMA shifts the T_g of PLLA to higher temperatures without losing transparency. The purpose of this study is to investigate the effect of CO_2 on

* Corresponding author.
E-mail address: msumita@o.cc.titech.ac.jp (M. Sumita).

0032-3861/$ - see front matter © 2006 Elsevier Ltd. All rights reserved.
doi:10.1016/j.polymer.2006.03.069

the crystallization behavior and the mechanical properties of PLLA/PMMA blends with various weight fraction of PMMA.

2. Experimental section

2.1. Blend sample preparation

PLLA was supplied from Toyota Motor Co. (LACTY #5000; $M_w = 320{,}000$). PMMA was provided from Mitsubishi Rayon Co., Ltd (Acrypet VH; $M_w = 100{,}000$). The blend samples with various weight fraction of PMMA were prepared by melt-blending at 180 °C for 15 min using a mixing roll. The quench films of 0.5 mm in thickness were obtained from the blend samples using a compression molding method at 180 °C under 19.6 MPa for 2 min followed by quenching into ice water.

2.2. Cold-crystallized sample

The cold-crystallized samples were obtained from the quenched films by annealing at 100 °C in air using a Mettler FP82 HT hot stage, followed by quenching into ice water.

2.3. CO_2 treated sample

The CO_2 treatment was conducted using the CO_2 extraction system (JASCO CO., Ltd) consisting of delivery pump (SFC-Get), automatic backpressure regulator (SCF-Bpg), and SUS-Ni alloy (Hastelloy) high-pressure reactor as shown in Fig. 1. The CO_2 treated films were prepared from the quenched films by treating with CO_2 at 0 °C for 1 h under a pressure of 10 MPa. It is emphasized that the beginning of the CO_2 treatment was decided as the time when the pressure in the reactor reached the setting pressure. After a period of CO_2 treatment, the reactor was quickly depressurized. The sample was set in the cold store at −1 °C for 72 h in order to avoid additional crystallization at room temperature because of the T_g depression. Afterwards the sample was vacuum evaporated at 30 °C for more than 1 week in order to remove the residual CO_2 in the sample. The re-annealed films were obtained from the CO_2 treated films by annealing at 80 °C for 1 h.

2.4. Measurements

The T_g, the melting temperature (T_m) and the heat of melting (ΔH_m) of the blends were measured by a Shimadzu Co. differential scanning calorimetry system consisting of a DSC-50 and a TA-50WS under nitrogen atmosphere at a heating rate of 20 °C min^{-1} from −20 to 220 °C. The degree of crystallinity of PLLA in the blend ($\chi_{c\,DSC}$) was obtained:

$$\chi_{c\,DSC}(\%) = \frac{\Delta H_m - \Delta H_c}{\Delta H_m^0} \frac{1}{W_{PLLA}} \times 100 \quad (1)$$

where ΔH_m^0, ΔH_m and ΔH_c are the heat of melting for the perfect crystalline PLLA (85.82 J g^{-1}), the heat of melting and the heat of crystallization of PLLA during the DSC heating run, respectively. The W_{PLLA} is the weight fraction of PLLA in the blend. Wide-angle X-ray diffraction (WAXD) measurements were carried out using a RINT-2100 (RIGAKU Co.) with Cu Kα radiation ($\lambda = 0.15418$ nm) and X-ray generator working at 40 kV, 40 mA. The optical system with pinhole geometry consists of a graphite monochromator and a scintillation counter. The intensity data were collected in the diffraction angle (2θ) range between 3 and 60°.

Small-angle X-ray scattering (SAXS) measurements were carried out using a Nano-Viewer (RIGAKU Co.). A Cu Kα radiation (40 kV, 20 mA) was generated by RA-Micro7 (RIGAKU Co.) and concentrated by Confocal MAX-Flux® (CMF) optic, which has the role as a monochromator ($\lambda =$ 0.15418 nm). The X-ray beam was collimated by a pinhole type slits. The two dimensional intensity data were detected using an imaging plate (IP) film (BAS-IP SR127, Fuji Photo Film Co., Ltd). The pinhole slits, sample, and IP film were set in a vacuum chamber and the two-dimensional scattering pattern was measured under a vacuum in order to eliminate air scattering. The distance between sample and IP film (camera length) was 482 mm, and the exposure time was set to 720 min. The two dimensional intensity data were read with a RINT-RAXIS-DS3 scanner (RIGAKU Co.). The one-dimensional profiles in the scattering angle (2θ) range between 0.2 and 3° were obtained by averaging the two dimensional data over 90 degrees in azimuth. The long period was estimated from the one-dimensional correlation function ($\gamma_1(x)$) defined as:

$$\gamma_1(x) = \frac{\int_0^\infty s^2 I(s)\cos(2\pi x s)\mathrm{d}s}{\int_0^\infty s^2 I(s)\mathrm{d}s} \quad (2)$$

where $I(s)$, s and x are the scattering intensity, the absolute value of the scattering vector ($= 2\sin(\theta/\lambda)$) and the correlation length, respectively.

Dynamic mechanical analysis (DMA) was conducted using DVA-200S (ITK Co.) in order to investigate the temperature dependence of storage modulus. The measurements were performed in a tension mode with a 0.1% strain amplitude at a frequency of 10 Hz. The temperature ranged from room temperature to 200 °C with a heating rate of 5 °C min^{-1}. For this measurement, the sample films were cut into rectangular specimens (30 mm × 5 mm × 0.5 mm). Tensile testing was performed on a UTM II-20 (Orientech Co.) with a crosshead speed of 4 mm min^{-1} at room temperature. The tensile specimens were cut into dumbell-shape with 2 mm in width, 20 mm in length and 0.5 mm in thickness. The estimation of a

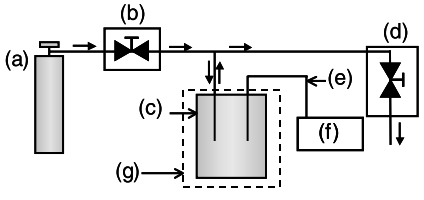

Fig. 1. Schematic diagram of CO_2 treatment apparatus; (a) CO_2 gas cylinder, (b) delivery pump, (c) high-pressure reactor, (d) automatic backpressure regulator, (e) thermocouple, (f) temperature monitor, (g) cooling bath.

transparency for the sample films was carried out using QV-2900 digital camera (Casio Computer Co., Ltd).

3. Results and discussion

3.1. Thermal properties of amorphous blend films

The DSC thermograms of quenched PLLA/PMMA blend films with different compositions are shown in Fig. 2. PLLA is the only crystallizable component in this system. In the curve of pure PLLA, an exothermic peak in the temperature range between 100 and 120 °C indicates the crystallization during the heating run. An endothermic peak around 175 °C proves the melting of PLLA crystals crystallized during the heating run. In the blends, the exothermic peak temperature shifts to higher temperatures and the peak intensity diminishes with increasing in PMMA weight fraction and the exothermic peak and the endothermic peak disappear in the blends containing above 40 wt% PMMA. This result indicates that PMMA inhibits the crystallization of PLLA. These quenched blend films are approximately amorphous independent of the compositions because the area of the exothermic peak and that of the endothermic peak are comparable in the blends containing below 30 wt% PMMA and both peaks are not detected in the blends containing above 40 wt% PMMA. The diffraction patterns with amorphous halo in WAXD profiles are also supports that the quenched blend films are amorphous as shown in Fig. 3. Therefore, we from this point on will describe the quenched films as the amorphous films.

The T_g of a polymer blend is one of the criteria for the miscibility of components. Fig. 4 shows the PMMA weight fraction dependence of the T_g values corresponding to those measured at the midpoint of the glass transition together with the values of ΔT_g, which is the temperature difference between the onset ($T_{g\ onset}$) and the endset ($T_{g\ endset}$) of the transition. The T_g of pure PLLA and pure PMMA are 62.6 and 120.6 °C, respectively, at a heating rate of 20 °C min^{-1}. The single T_g is observed between those of the pure polymers and the T_g of the blend rises monotonically with increasing the PMMA weight

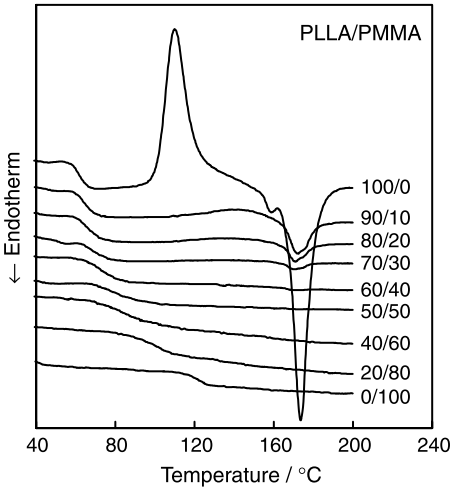

Fig. 2. DSC thermograms of quenched PLLA/PMMA blends.

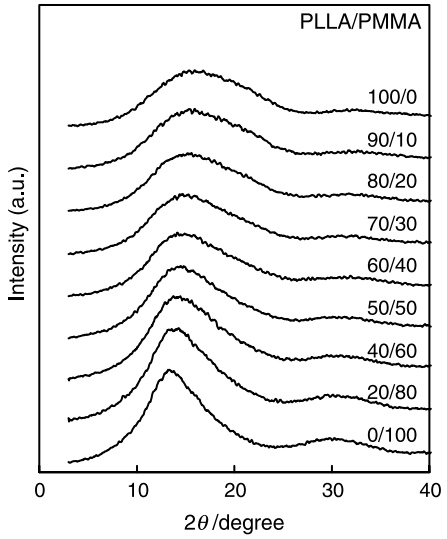

Fig. 3. WAXD curves of quenched PLLA/PMMA blends.

fraction. For miscible polymer blend system, a number of equations have been proposed to describe the composition dependence of the T_g of the blend. The Gordon–Taylor equation has been one of the most frequently used [3]:

$$T_g = T_{g1} + \frac{kW_2(T_{g2} - T_{g1})}{W_1 + kW_2} \tag{3}$$

where W_i refers to the weight fraction of component i and T_{gi} is its glass transition temperature. Subscripts 1 and 2 represent PLLA and PMMA in this article. The fitting parameter k is obtained by applying Eq. (3) to the experimental results and a value of $k=0.366$ is suitable for this blend system. These results indicates that PLLA/PMMA blend is miscible in the glassy state. However, the glass transition width, ΔT_g ($=T_{g\ endset} - T_{g\ onset}$) is wider for the blends than that of the pure PLLA and PMMA. The maximum ΔT_g is found in the blends containing 50 wt% PMMA. Huang et al. [4] studied on the miscibility of poly(tetramethylene terephthalate) (PTT)/

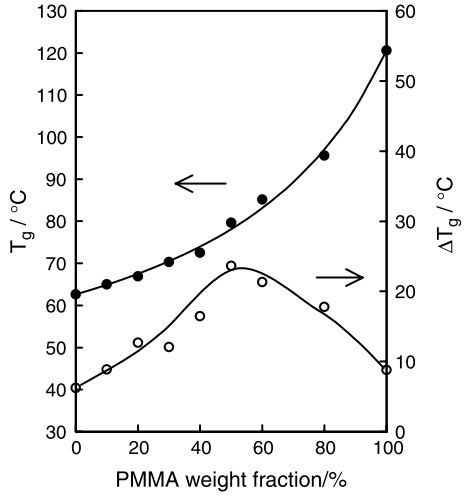

Fig. 4. PMMA weight fraction dependence of T_g and the glass transition width (ΔT_g) for amorphous PLLA/PMMA blends.

poly(ether imide) (PEI) blends and reported the similar results, in which the ΔT_g exhibits a maximum at the intermediate blend composition. They concluded that the widenings in the glass transition were attributed to local compositional microheterogeneity based on the idea of MacKnight et al. [5]. Therefore, we determine that the PLLA/PMMA blend is miscible in the glassy state although that has a compositional fluctuation at the intermediate blend composition.

3.2. Crystallization behavior and crystal form of PLLA/PMMA blends

The DSC thermograms of the blend films cold-crystallized at 100 °C for 24 h are shown in Fig. 5. The treatment period was set long enough that the crystallinity of PLLA/PMMA 50/50 film, which had the slowest crystallization rate among these samples, leveled off. In the curve of pure PLLA, there is an endothermic peak with the T_m of about 175 °C. The area of endothermic peak decreases and the T_m shifts slightly to lower temperatures with increasing the weight fraction of PMMA. The decrease in the T_m is attributed to the presence of PMMA molecules as a heterogeneous component in the amorphous phase near the PLLA lamellae [6]. Fig. 6 shows the WAXD curves of the cold-crystallized blend films. The diffraction peaks at 16.7 and 19.3° are observed in the profile of the pure PLLA cold-crystallized film and they are attributed to the (110)/(200) and (203) plane of α-form, respectively [7]. The intensity of these diffraction peaks decreases with an increase in the weight fraction of PMMA but the peaks keep each position. Therefore, the crystal form of PLLA in the PLLA/PMMA blends also have the α-form as well as the pure PLLA. From above discussion, it is considered that PMMA molecules segregate from the PLLA lamellar region during the annealing and they were present mixed with the amorphous PLLA molecules beside the PLLA lamellae.

Fig. 7 shows the DSC thermograms of the PLLA/PMMA blend films treated with high-pressure CO_2 at 0 °C for 1 h under a pressure of 10 MPa. The degree of crystallinity for PLLA in the blend leveled off within 1 h though the crystallization rate of PLLA in the blend decreases with increasing the weight fraction of PMMA as well as the cold-crystallization. The endothermic peak with the T_m of 174 °C is observed in the curve of the pure PLLA and the T_m of the curves for the blends shifts to lower temperatures with increasing the weight fraction of PMMA. These results are similar to those of cold-crystallized films. The WAXD curves of CO_2 treated films are shown in Fig. 8. The diffraction peaks of the pure PLLA film treated with high-pressure CO_2 are much broader than those of the cold-crystallized PLLA film. Asai et al. found that the crystal structure developed during the high-pressure CO_2 treatment at a low temperature was disordered compared to that of the cold-crystallized film [8]. They also reported that the disordered structure of the CO_2 treated film was rearranged into

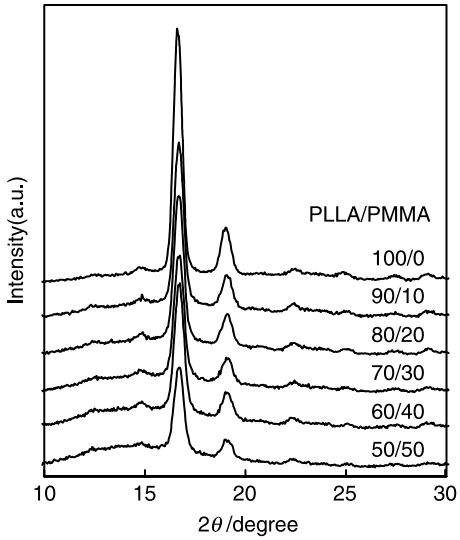

Fig. 6. WAXD curves of PLLA/PMMA blends cold-crystallized at 100 °C for 24 h.

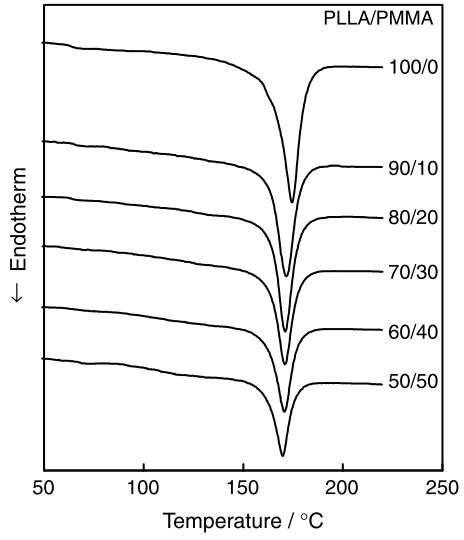

Fig. 5. DSC thermograms of PLLA/PMMA blends cold-crystallized at 100 °C for 24 h.

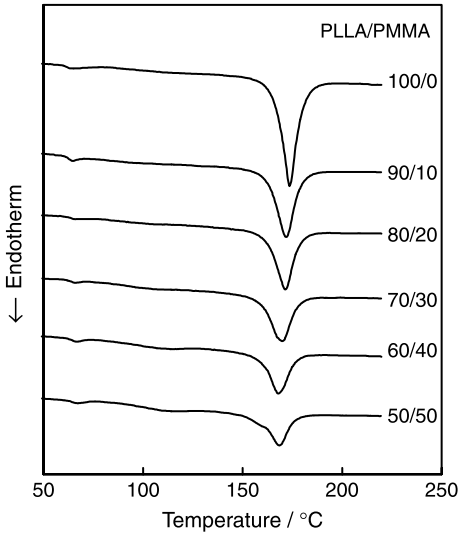

Fig. 7. DSC thermograms of PLLA/PMMA blends treated with CO_2 at 0 °C under a pressure of 10 MPa for 1 h.

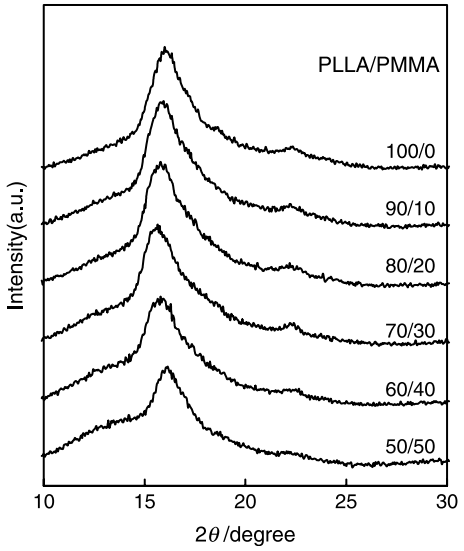

Fig. 8. WAXD curves of PLLA/PMMA blends PLLA/PMMA blends treated with CO_2 at 0 °C under a pressure of 10 MPa for 1 h.

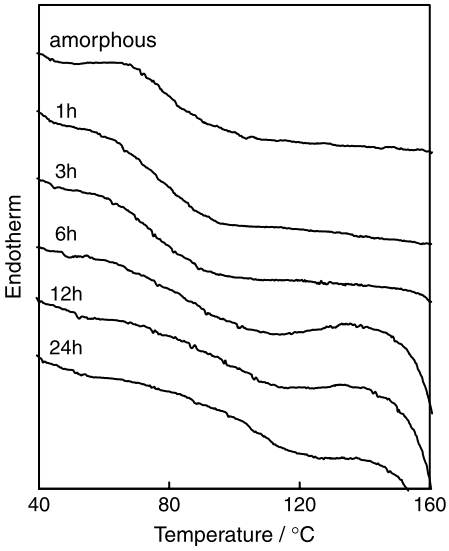

Fig. 10. Annealing time dependence of the DSC curves for PLLA/PMMA 50/50 blend during annealing at 100 °C in air.

the α-form by re-annealing at 80 °C. As the diffraction pattern of the blend films is comparable to that of the pure PLLA, the crystal form developed in the blends during the CO_2 treatment is a disordered form like that of the pure PLLA film.

3.3. The degree of crystallinity for PLLA in PLLA/PMMA blends

Fig. 9 shows the degree of crystallinity for PLLA in the blends ($\chi_{c\ DSC}$) obtained from the DSC thermograms of cold-crystallized and CO_2 treated films. The $\chi_{c\ DSC}$ is normalized with the weight fraction of PLLA. The $\chi_{c\ DSC}$ of blends have values lower than that of the pure PLLA independently of the process of the crystallization. Blending PMMA inhibits the crystallization of PLLA in the blends. However, the values of $\chi_{c\ DSC}$ for the blends stay constant from 10 to 50 wt% PMMA. The PLLA molecules are diluted with increasing the weight fraction of PMMA. The progression of the crystallization of PLLA in the blends leads to an increase in PMMA concentration and an increase in the T_g in the miscible amorphous phase because the PMMA molecules segregate from the PLLA lamellar region. It is expected that $\chi_{c\ DSC}$ decreases with increasing the weight fraction of PMMA from these factors, however, this expectation is conflict with the result showed in Fig. 9. The maximum glass transition width (ΔT_g) is found in the amorphous blends containing 50 wt% PMMA. Therefore, the compositional fluctuation in the amorphous blend becomes larger with an increase in the weight fraction of PMMA up to 50 wt% PMMA. It seems that the crystallization tends to occur in the PLLA-rich domains.

Fig. 10 displays the annealing time dependence of the DSC curves for PLLA/PMMA 50/50 blend during anneling at 100 °C in air. It is seen that the glass transition region varies with increasing an anneling time. Fig. 11 shows the annealing time (t_a) dependence of the $T_{g\ onset}$ and $\chi_{c\ DSC}$ of the PLLA/PMMA 50/50 blend film during annealing at 100 °C in air. It is

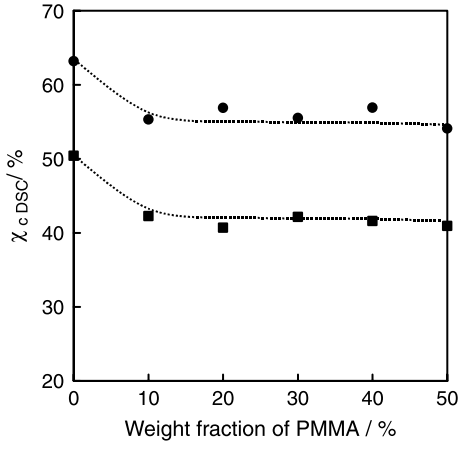

Fig. 9. The degree of crystallinity for PLLA in PLLA/PMMA blends; cold-crystallized at 100 °C for 24 h (filled circles) and treated with CO_2 at 0 °C for 1 h under a pressure of 10 MPa (filled squares).

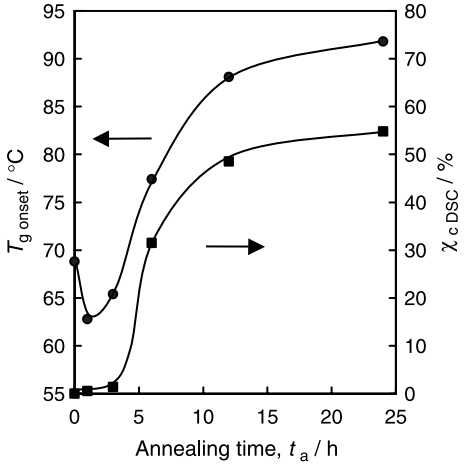

Fig. 11. Annealing time dependence of the T_g (filled circles) and the $\chi_{c\ DSC}$ (filled squares) of PLLA/PMMA 50/50 blend film during annealing at 100 °C.

found that the $\chi_{c\ DSC}$ stays constant, while the $T_{g\ onset}$ shifts to lower temperatures up to $t_a = 3$ h. It appears that the PLLA content is enriched in some amorphous regions at the initial stage of the annealing. The increase in the $T_{g\ onset}$ with increasing the $\chi_{c\ DSC}$ is attributed to a decrease in the amorphous PLLA molecules in the PLLA-rich domains. Therefore, the compositional fluctuation in the amorphous blend and the phase separation at the initial stage of the annealing lead to the crystallization of PLLA in the blends containing relatively high weight fraction of PMMA. It seems that the crystallization of PLLA in the blends under high-pressure CO_2 is also via the phase separation as well as the cold-crystallization.

3.4. Higher-order structure of PLLA and PLLA/PMMA blends

CO_2 treated films have a disordered crystal structure as mentioned above. The CO_2 treated films were re-annealed at 80 °C for 1 h in order to eliminate the disorder for the analysis of the higher-order structure of the CO_2 treated films. Fig. 12 shows the long period of cold-crystallized and re-annealed films. The long period was defined as the first maximum of the one-dimensional correlation function derived from the SAXS profile. The first maximum of the function for the blends containing above 10 wt% PMMA could not be obtained because the scattering peak position gets close to the lower limit of the measurable angular range in the SAXS profile. Consequently, the PLLA/PMMA blends with the small weight fraction of PMMA (3, 5 wt%) were prepared in order to estimate the PMMA weight fraction dependence of the long period. The values of the long period for CO_2 treated films are smaller than that for the cold-crystallized films. Asai et al. reported that the treatment temperature is a main factor for the higher-order structure of poly(ethylene 2,6-naphthalate) (PEN) film which is crystallized by $scCO_2$ treatment [1]. The long period of $scCO_2$-treated PEN film decreased with decreasing the treatment temperature. To return the PLLA/PMMA blends, the long period of the CO_2 treated films becomes short because

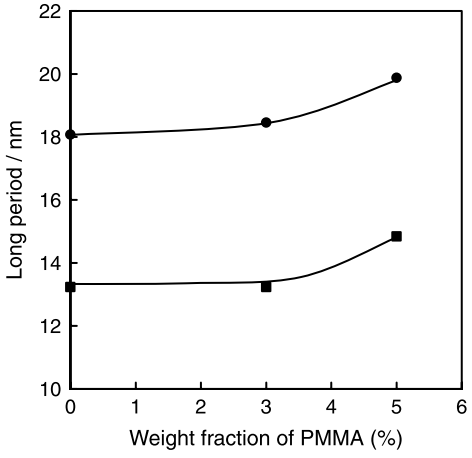

Fig. 12. Long period of PLLA and PLLA/PMMA blends; cold-crystallized at 100 °C for 24 h (filled circles) and re-annealed at 80 °C for 1 h after the CO_2 treatment at 0 °C for 1 h under a pressure of 10 MPa (filled squares).

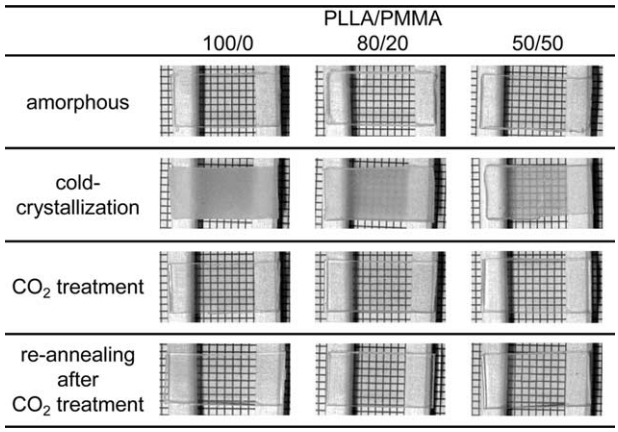

Fig. 13. Photographs of PLLA and PLLA/PMMA blends; amorphous, cold-crystallized at 100 °C for 24 h, treated with CO_2 at 0 °C for 1 h under a pressure of 10 MPa and re-annealed after CO_2 treatment.

the temperature of the CO_2 treatment is 100 °C lower than that of the cold-crystallization. Moreover, the value of the long period increases with increasing the weight fraction of PMMA independently of the treatments. This is because the PMMA molecules segregate to the interlamellar region during the crystallization of PLLA in the blends and remain in the interlamellar region in the PLLA lamellar stack.

3.5. Evaluation of transparency for amorphous and crystallized PLLA/PMMA blends

Fig. 13 shows the photographs of the amorphous, cold-crystallized, CO_2 treated and re-annealed PLLA/PMMA blend films. The amorphous films have a good transparency regardless of the composition. The translucence or opaqueness of the cold-crystallized films is due to the scattering of visible light by the spherulite of PLLA in the films. On the other hand, the CO_2 treated films have a good transparency, even though these films contain the PLLA crystals. It is considered that the size of the aggregation for the lamellar stacks, which were

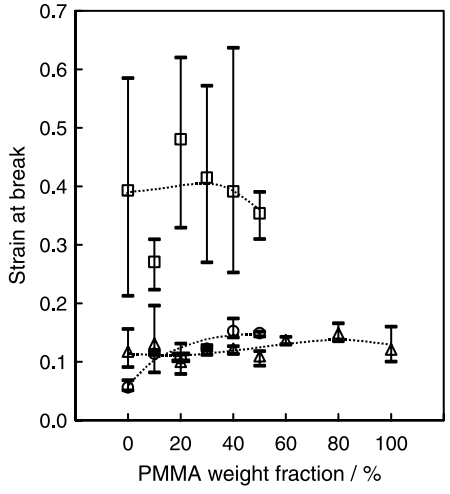

Fig. 14. Strain at break of PLLA and PLLA/PMMA blends; amorphous (open triangles), cold-crystallized at 100 °C for 24 h (open circles) and treated with CO_2 at 0 °C for 1 h under a pressure of 10 MPa (open squares).

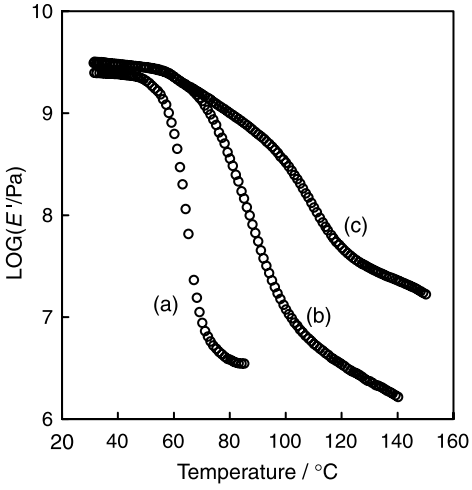

Fig. 15. Temperature dependence of storage modulus of amorphous PLLA (a) amorphous PLLA/PMMA 50/50 blends (b) and treated with CO_2 at 0 °C for 1 h under a pressure of 10 MPa (c).

developed during the high-pressure CO_2 treatment at 0 °C under a pressure of 10 MPa, is smaller than the wavelength of the visible light. Moreover, the films re-annealed at 80 °C for 1 h following the CO_2 treatment have a good transparency.

3.6. Mechanical properties of amorphous and crystallized PLLA/PMMA blends

Fig. 14 shows the PMMA weight fraction dependence of the strain at break of the amorphous, cold-crystallized, and CO_2 treated PLLA/PMMA blend films. The CO_2 treated films have about three times larger strain at break than that of the amorphous and cold-crystallized films. The size of the aggregations for PLLA lamellar stacks in the CO_2 treated films seems to be small enough to have a good transparency. The improvement of the strain at break is attributed to the reduction of the stress concentration during the deformation. Compared to the amorphous films, the small and dispersed aggregations of PLLA lamellar stacks in the CO_2 treated films work as the cross-linking points, which is responsible for the improvement of the elongation at break.

The temperature dependence of the storage modulus for amorphous PLLA film, amorphous PLLA/PMMA 50/50 film, and CO_2 treated PLLA/PMMA film are summarized in Fig. 15. Blending PLLA and PMMA, which has the T_g higher than that of PLLA, shifts the softening temperature to higher temperatures. In addition, the crystallization of PLLA in the blend by the CO_2 treatment leads to a inhibition of the decrease in the storage modulus at temperatures above the T_g. Although the similar result can be obtained in the cold-crystallized PLLA/PMMA 50/50 film, the CO_2 treated film is excellent in terms of a good transparency and a large elongation at break.

4. Conclusions

The crystallization behavior and the mechanical properties of the cold-crystallized PLLA/PMMA blend films were studied as well as those of the CO_2 treated films. The PLLA/PMMA blend films are miscible in the amorphous state, although the blends have local compositional microheterogeneity. The crystal form of PLLA crystallized in the PLLA/PMMA blends is the same as that of the pure PLLA. The PMMA molecules segregate to the interlamellar region during the crystallization of PLLA in the blends and remain in the interlamellar region in the PLLA lamellar stack. The phase separation at the initial stage of the crystallization leads to the crystallization of PLLA in the blends containing relatively high weight fraction of PMMA. The long period of the CO_2 treated films are small values compared to that of the cold-crystallized films. Moreover, the CO_2 treated pure PLLA and the blends have a good transparency and have about three times larger strain at break than those of the amorphous and the cold-crystallization films. The reason seems to be that the size of the aggregation of the crystalline lamellae is smaller than the wavelength of the visible light. Finally, blending PLLA and PMMA and CO_2 treatment at a low temperature lead to the improvement of a heat resistance and flexibillity without losing a transparency.

References

[1] Asai S, Shimada Y, Tominaga Y, Sumita M. Macromolecules 2005;38:6544–50.
[2] Zhang G, Zhang J, Wang S, Shen D. J Polym Sci, Part B: Polym Phys 2003;41:23–30.
[3] Gordon M, Taylor JS. J Appl Chem 1952;2:493–500.
[4] Huang J, Chang F. J Appl Polym Sci 2002;84:850–6.
[5] MacKnight WJ, Karasz FE, Fried JR. Solid state transition behavior of blends. In: Paul DR, Newman S, editors. Polymer blends. New York: Academic Press; 1978 [chapter 5].
[6] Nishi T, Wang TT. Macromolecules 1975;8:909–15.
[7] Hoogsteen W, Postema AR, Pennings AJ, Brinke GT. Macromolecules 1990;23:634–42.
[8] Asai S, Ikura Y, Tominaga Y, Sumita M. Eighth European symposium on polymer blends, Bruges, Belgium; 2005.